Probing the soft rescattering parameters in B decays

Based on Physical Review D 111, 016017 (2025)

祁敬娟[a]

合作者：张振华、王振洋、魏科伟、郭新恒

[a] 浙江万里学院

全国重味物理和CP破坏研讨会　北京

2025年10月25日

Background

- In 2013 and 2014, LHCb found evidence of inclusive integrated CP asymmetries in B decays, using an integrated luminosity of 3.0 fb^{-1} (Fig 1);

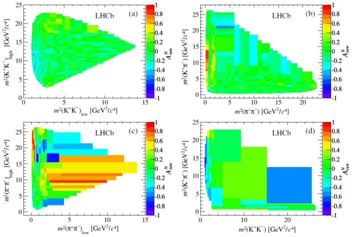

图 1 Measured A^N_{raw} in Dalitz plot bins of background-subtracted and acceptance-corrected events for B three-body decays, Phys. Rev. D 90, 112004 (2014).

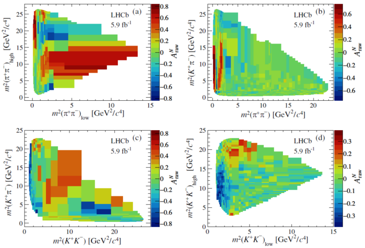

图 2 Asymmetry distribution in bins of the Dalitz plot for B three-body decays, Phys. Rev. D 108, 012008 (2023).

- In 2024, LHCb conducted more refined investigations, using an integrated luminosity of 5.9 fb^{-1} (Fig 2);

- In 2020, LHCb found a large CP asymmetry related to the interference between the $S-$ and $P-$ wave contributions in $B^{\pm} \longrightarrow \pi^{\pm}\pi^{+}\pi^{-}$ decays;

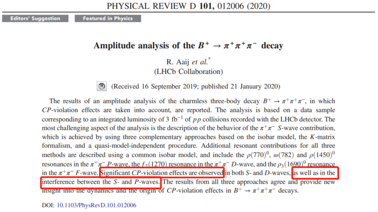
PHYSICAL REVIEW D **101,** 012006 (2020)

Editors' Suggestion | Featured in Physics

Amplitude analysis of the $B^+ \to \pi^+\pi^+\pi^-$ decay

R. Aaij *et al.*[*]
(LHCb Collaboration)

(Received 16 September 2019; published 21 January 2020)

The results of an amplitude analysis of the charmless three-body decay $B^+ \to \pi^+\pi^+\pi^-$, in which CP-violation effects are taken into account, are reported. The analysis is based on a data sample corresponding to an integrated luminosity of 3 fb^{-1} of pp collisions recorded with the LHCb detector. The most challenging aspect of the analysis is the description of the behavior of the $\pi^+\pi^-$ S-wave contribution, which is achieved by using three complementary approaches based on the isobar model, the K-matrix formalism, and a quasi-model-independent procedure. Additional resonant contributions for all three methods are described using a common isobar model, and include the $\rho(770)^0$, $\omega(782)$ and $\rho(1450)^0$ resonances in the $\pi^+\pi^-$ P-wave, the $f_2(1270)$ resonance in the $\pi^+\pi^-$ D-wave, and the $\rho_3(1690)^0$ resonance in the $\pi^+\pi^-$ F-wave. Significant CP-violation effects are observed in both S- and D-waves, as well as in the interference between the S- and P-waves. The results from all three approaches agree and provide new insight into the dynamics and the origin of CP-violation effects in $B^+ \to \pi^+\pi^+\pi^-$ decays.

DOI: 10.1103/PhysRevD.101.012006

图 3 The abstract of Phys.Rev.D 101, 012006 (2020).

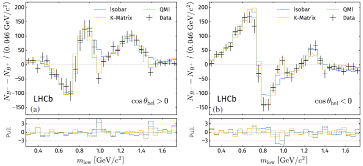

图 4 Raw difference in the number of B^- and B^+ candidates in the low-$m_{\pi\pi}$ region, for (a) positive, and (b) negative cosine of the helicity angle, Phys.Rev.D 101, 012006 (2020).

Consider the interfenence of the $\rho(770)^0$ and $S-$ wave resonance (such as $f_0(500)$), thus the total amplitude can be written as

$$A_{total} = A_\rho + A_f e^{i\delta_{f_0(500)}},$$
$$= \frac{A_\rho^{\rm weak} A_\rho^{\rm strong}}{S_\rho} + \frac{A_f^{\rm weak} A_f^{\rm strong}}{S_f} e^{i\delta_{f_0(500)}}$$

where $A_\rho^{\rm weak}$ and $A_f^{\rm weak}$ can be addressed with the QCDF.

Motivation

In order to test the relationships between the X_k^{SP} and X_k^{PS} for $B \to \sigma/f_0(500)$ decay

- ? $X_k^{SP} = X_k^{PS}$.
- ? $\rho_k^{SP/PS} \leq 1.$

A review of theoretical approaches

- Factorization Approach： H. Y. Cheng, C. K. Chua, Y. Li,⋯
- PQCD： H. n. Li, C. D. Lü, Z. J. Xiao, W. Wang, W. F. Wang, R. Zhou, Y. Li ...
- Symmetry： X. G. He, G. N. Li, D. Xu, J. L. Rosner, M. Gronau...
- Sum rules： Ulf-G. Meiβner, Y. M. Wang, Y. L. Sheng, S. Cheng, A. Khodjamirian...
- QCD Factorization： M. Beneke, M. Neubert, A. Furman, B. El Bennich, R. Kaminski, T. Mannel, H.Y. Cheng, X. H. Guo, Y. D. Yang, Q. Chang, J. F. Sun, X.Q. Li, Z. H. Zhang...

End-point divergency QCDF

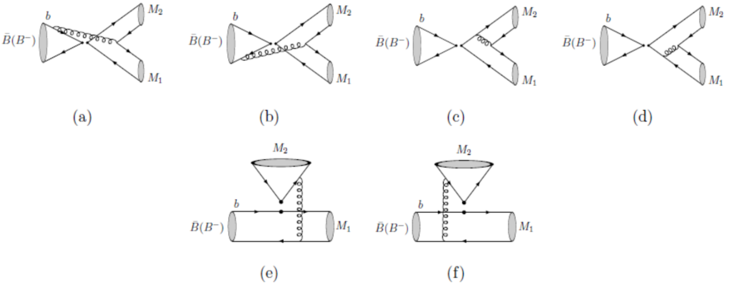

图 5 The lowest order diagrams of weak annihilation (a-d) and spectator scattering (e,f) [from Phys.Rev.D 90 (2014) 5, 054019].

End-point divergency QCDF

- Regulation Scheme(parameterization)

for the hard-spectator scatterings:

$$\int_0^1 \frac{dx}{\bar{x}} \to X_H;$$

for the weak-annihilation parts:

$$\int_0^1 \frac{dx}{x} \to X_A, \quad \int_0^1 dx \frac{lnx}{x} \to -\frac{1}{2}(X_A)^2,$$

and

$$X_H = X_A = X_k = (1 + \rho_k e^{i\phi_k}),$$

- Traditional scenarios

$$\rho_k \leq 1, \quad \text{and} \quad \phi_k \in [0, 2\pi].$$

Brief summary of the “new” treatment

More detailed analysis

- the values of ρ and ϕ for $B \to PV/PV$ are different $X^{PV} \neq X^{VP}$;
  H. Y. Cheng and C. K. Chua, Phys. Rev. D 80, 114008 (2009)......
- X_A^i is possibly non-universal for $B_{u,d}$ and B_s decays, but X_A^f is universal, since the flavor asymmetry-breaking effects.
  Guo-Huai Zhu, Phys. Lett. B 702 (2011) 408; Kai Wang and Guo-Huai Zhu, Phys. Rev. D 88 (2013) 014043......
- $X_A^i \neq X_A^f$ is possible due to gluon emission from the initial and final state quarks, respectively.
  Qin Chang, Junfeng Sun, Yueling Yang, Xiaonan Li Phys.Rev.D 90 (2014) 5, 054019.......

Test the relationships between X_k^{SP} and X_k^{PS}

In order to test the relationships between the X_k^{SP} and X_k^{PS} for $B \to \sigma/f_0(500)$ decay

- ? $X_k^{SP} = X_k^{PS}$.
- ? $\rho_k^{SP/PS} \leq 1$.

The inner structure of the scalar (S) mesons

The structure of the S meson has been studied for a long time, and now it is still a hot topic.

- There are several explanations, e.g., $q\bar{q}$ state, tetraquark states, molecule states, glueball and hybrid states, while there is still no general agreement.

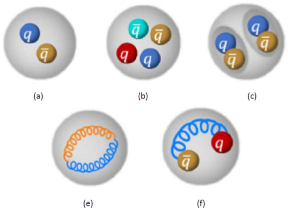

图 6 The possible interpretations of scalar mesons, (a-c) are $q\bar{q}$, tetraquark state, molecular state and (e-f)) are glueball state and hybrid state from left to right, respectively.

The inner structure of the scalar (S) mesons

For the light scalar mesons

In the 2-quark mode

- the scalar mesons with mass below 1 GeV are form a SU(3) nonet, such as $\sigma/f_0(500)$, $f_0(980)$, $a_0(980)$, $K_0^*(700)/\kappa$;
- the ones with mass above 1 GeV are classified into another SU(3) nonet, such as $f_0(1370)$, $f_0(1500)$, $a_0(1450)$, $K_0^*(1430)$.

In the tetraquark mode (favored by lattice calculations)

- the former are predominately the $qq\bar{q}\bar{q}$ states without introducing a unit of orbital angular momentum;
- the latter are treated as the lowest lying $q\bar{q}$ p-wave states.

LCPA, FBA and FBA-CPA

The definition of θ

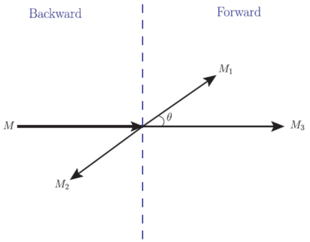

图 7 The definition of θ in the c.m. frame of the $M_1 M_2$ system (M is chosen to be the B meson).

$$\cos\theta = \frac{\vec{p}_1^{\,*} \cdot \vec{p}_3^{\,*}}{|\vec{p}_1^{\,*}||\vec{p}_3^{\,*}|} \tag{1}$$

where $\vec{p}_j^{\,*}$ is the momentum of M_j in the c.m. frame of the $M_1 M_2$ system.

LCPA, FBA and FBA-CPA

The introductions of the concepts

- LCPA: Localized CP asymmetry,

$$\mathcal{A}_{CP}^{L} = \frac{N_{B^-}(\text{Forward} + \text{Backward}) - N_{B^+}(\text{Forward} + \text{Backward})}{N_{B^-}(\text{Forward} + \text{Backward}) + N_{B^+}(\text{Forward} + \text{Backward})}, \quad (2)$$

- FBA: Forward-backward asymmetry,

$$\mathcal{A}_{FB} = \frac{N_{B^\mp}(\text{Forward}) - N_{B^\mp}(\text{Backward})}{N_{B^\mp}(\text{Forward}) + N_{B^\mp}(\text{Backward})}, \quad (3)$$

- FBA-CPA: Forward-backward asymmetry induced CP asymmetry,

$$\mathcal{A}_{FB}^{CP} = \frac{1}{2}(\mathcal{A}_{FB} - \bar{\mathcal{A}}_{FB}), \quad (4)$$

Advantage of the FBA-CPA

Supplement

- One is that can isolate CPV caused by the interference from the nearby resonances,
  arXiv:2410.08539v2, Eur.Phys.J.C 83 (2023) 2, 133, Phys.Rev.D 106 (2022) 11, 113002, Phys.Rev.D 105 (2022) 9, 093007......

  for example: Phys. Rev. D 105 (2022) 9, 093007, Rui Hu and Zhang Zhen-Hua, $m_{KK} \approx 1.5$ GeV, the large FBA can be explained by the interference of the resonances with even and odd spins, such as $\rho(1450)^0$ and $f_0(1500)$.

- Another is that can investigate the contributions of the real and imaginary parts in the interference term to the relevant physical quantities,
  Phys.Rev. D 110 (2024) 11, L111301......

For example

- Consider the interference of the V and S mesons, such as $\rho(770)^0$ and $f_0(500)$, the amplitude is

$$A_{total} = A_\rho + A_f e^{i\delta_{f_0(500)}} \propto F(\rho_k^{SV}, \phi_k^{SV}, \rho_k^{VS}, \phi_k^{VS}, \delta_{f_0(500)}),$$

- The event yield of each bin i, $N_{B^\pm,i}$ has the following form

$$N_{B^\pm,i} = \eta \int_{\cos\theta \gtrless 0} R|A_{total}|^2_{m_{12}=m_{12,i}} d\cos\theta,$$

where η is the ratio of the total number of events to the total decay width and R is the phase-space factor with the form

$$R = \sqrt{(m_{12}^2 - 4m_{M_2}^2)[m_B^2 - (m_{12} - m_{M_3})^2][m_B^2 - (m_{12} + m_{M_3})^2]}.$$

Thus,

$$N_{B^\pm,i} \propto F'(\eta, \rho_k^{SV}, \phi_k^{SV}, \rho_k^{VS}, \phi_k^{VS}, \delta_{f_0(500)}).$$

For example

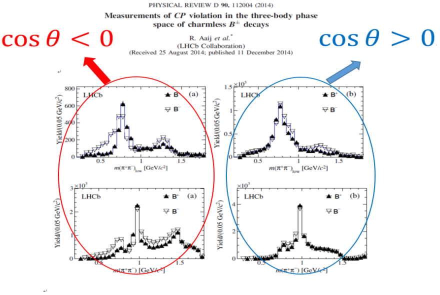

Bin (GeV)	$B^{\pm}\to\pi^{\pm}\pi^{+}\pi^{-}$ $N_i(\cos\theta>0)$	$N_i(\cos\theta<0)$	$\bar{N}_i(\cos\theta>0)$	$\bar{N}_i(\cos\theta<0)$	$B^{\pm}\to K^{\pm}\pi^{+}\pi^{-}$ $N_i(\cos\theta>0)$	$N_i(\cos\theta<0)$	$\bar{N}_i(\cos\theta>0)$	$\bar{N}_i(\cos\theta<0)$
0.445–0.495	139 ± 12	112 ± 11	108 ± 10	48 ± 7	89 ± 9	197 ± 14	20 ± 4	34 ± 6
0.495–0.545	153 ± 12	152 ± 12	148 ± 12	38 ± 6	49 ± 7	226 ± 15	20 ± 4	64 ± 8
0.545–0.595	159 ± 13	165 ± 13	182 ± 13	48 ± 7	89 ± 9	244 ± 16	20 ± 4	76 ± 9
0.595–0.645	196 ± 14	263 ± 16	265 ± 16	60 ± 8	158 ± 13	358 ± 19	89 ± 9	128 ± 11
0.645–0.695	368 ± 19	302 ± 17	446 ± 21	130 ± 11	227 ± 15	539 ± 23	236 ± 15	202 ± 14
0.695–0.745	721 ± 27	473 ± 22	813 ± 29	321 ± 18	719 ± 27	815 ± 29	660 ± 26	388 ± 20
0.745–0.795	1140 ± 34	472 ± 22	1089 ± 33	623 ± 25	1172 ± 34	856 ± 29	1005 ± 32	496 ± 22

图 7 The event yields for $B^{\pm}\to\pi^{\pm}\pi^{+}\pi^{-}$ and $B^{\pm}\to K^{\pm}\pi^{+}\pi^{-}$ decays with $m_{\pi\pi}$ ranging from 0.445 GeV to 0.795 GeV based on Figs. 4 and 5 in Ref. Phys. Rev. D 108, 012008 (2023), where $N_i(\cos\theta\gtrless 0)$ and $\bar{N}_i(\cos\theta\gtrless 0)$ for $B^-\to\pi^-(K^-)\pi^+\pi^-$ and $B^+\to\pi^+(K^+)\pi^+\pi^-$ decays, respectively, and the uncertainties are statistical only.

Fitted results

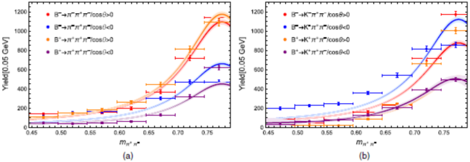

图 8 The fitted curves for the (a) $B^{\pm} \to \pi^{\pm}\pi^{+}\pi^{-}$ and (b) $B^{\pm} \to K^{\pm}\pi^{+}\pi^{-}$ decays, the event yields are from the data of LHCb. The contribution only from the $\rho(770)^0$ resonance.

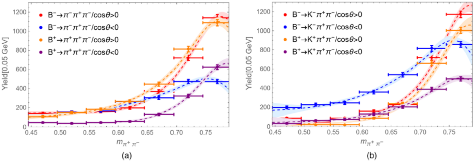

图 9 The fitted curves for the (a) $B^{\pm} \to \pi^{\pm}\pi^{+}\pi^{-}$ and (b) $B^{\pm} \to K^{\pm}\pi^{+}\pi^{-}$ decays, the event yields are from the data of LHCb. The contribution from the $\rho(770)^0$ and $f_0(500)$ are considered in our theoretical calculations.

Fitted results and comparisons

- Fitted results

$$\begin{cases} |\rho_k^{SP}| = 3.29 \pm 1.01, & |\phi_k^{SP}| = 0.85 \pm 0.31; \\ |\rho_k^{PS}| = 2.33 \pm 0.73, & |\phi_k^{PS}| = 0.15 \pm 0.08; \\ \delta_{f_0(500)} = 0.85 \pm 0.39, & \eta = (2.47 \pm 0.83)\mathrm{GeV}^{-1}. \end{cases}$$

- Consistency check (for $\mathcal{A}_{FB}^{CP}$ and $\mathcal{A}_L^{CP}$ for $B^\pm \to \pi^\pm\pi^+\pi^-$ and $B^\pm \to K^\pm\pi^+\pi^-$ decays, respectively)

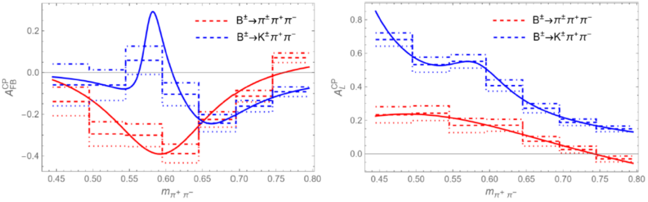

(a) (b)

$|\rho_k| > 1$ means the contributions from the annihilation and hard-scattering processes are relatively significant.

- Investigations into CPVs have been continuously pursued both in experimental and theoretical aspects;
- End-point divergency parameters X_k in QCDF require non-traditional treatments;
- The interference between different resonance (such as S- and P- wave, P- and D-wave) should not be overlooked in the studies of LCPVs, FBAs and FBA-CPAs.

Thanks!